Cardiovascular Research (2009) **81**, 528–535
doi:10.1093/cvr/cvn290

Expression of skeletal but not cardiac Na^+ channel isoform preserves normal conduction in a depolarized cardiac syncytium

Lev Protas[1], Wen Dun[1], Zhiheng Jia[5], Jia Lu[4], Annalisa Bucchi[1], Sindhu Kumari[4], Ming Chen[1], Ira S. Cohen[4,6], Michael R. Rosen[1,2,3], Emilia Entcheva[4,5,6], and Richard B. Robinson[1,3]*

[1]*Department of Pharmacology, College of Physicians and Surgeons, Columbia University, 630 West 168 Street, Room PH7West-318, New York, NY 10032, USA;* [2]*Department of Pediatrics, College of Physicians and Surgeons, Columbia University, New York, NY, USA;* [3]*The Center for Molecular Therapeutics, College of Physicians and Surgeons, Columbia University, New York, NY, USA;* [4]*Department of Physiology and Biophysics, Stony Brook University, Stony Brook, NY, USA;* [5]*Biomedical Engineering, Stony Brook University, Stony Brook, NY, USA; and* [6]*Institute for Molecular Cardiology, Stony Brook University, Stony Brook, NY, USA*

Received 6 August 2008; revised 4 October 2008; accepted 24 October 2008; online publish-ahead-of-print 31 October 2008

Time for primary review: 25 days

KEYWORDS
Na^+ channel;
Gene therapy;
Arrhythmia;
Conduction;
Mapping

Aims Reentrant arrhythmias often develop in the setting of myocardial infarction and ensuing slow propagation. Increased Na^+ channel expression could prevent or disrupt reentrant circuits by speeding conduction if channel availability is not limited by membrane depolarization within the diseased myocardium. We therefore asked if, in the setting of membrane depolarization, action potential (AP) upstroke and normal conduction can be better preserved by the expression of a Na^+ channel isoform with altered biophysical properties compared to the native cardiac Na^+ channel isoform, namely having a positively shifted, voltage-dependent inactivation.

Methods and results The skeletal Na^+ channel isoform (SkM1) and the cardiac Na^+ channel isoform (Nav1.5) were expressed in newborn rat ventricular myocyte cultures with a point mutation introduced in Nav1.5 to increase tetrodotoxin (TTX) sensitivity so native and expressed currents could be distinguished. External K^+ was increased from 5.4 to 10 mmol/L to induce membrane depolarization. APs, Na^+ currents, and conduction velocity (CV) were measured. In control cultures, elevated K^+ significantly reduced AP upstroke ($\sim$75%) and CV ($\sim$25%). Expression of Nav1.5 did not protect AP upstroke from K^+ depolarization. In contrast, in SkM1 expressing cultures, high K^+ reduced AP upstroke $<$50% and conduction was not significantly reduced. In a simulated anatomical reentry setting (using a void), the angular velocity (AV) of induced reentry was faster and the excitable gap shorter in SkM1 cultures compared to control for both normal and high K^+.

Conclusion Expression of SkM1 but not Nav1.5 preserves AP upstroke and CV in a K^+-depolarized syncytium. The higher AV and shorter excitable gap observed during reentry excitation around a void in SkM1 cultures would be expected to facilitate reentry self-termination. SkM1 Na^+ channel expression represents a novel gene therapy for the treatment of reentrant arrhythmias.

1. Introduction

Infarct-associated ventricular tachycardia is usually reentrant in nature[1,2] and its onset depends on local propagation speed, refractoriness, and, hence, pathlength available for the reentrant circuit. Existing pharmacologic therapies largely focus on decreasing conduction velocity (CV) and/or prolonging refractoriness, and their global action can lead to potentially pro-arrhythmic effects in healthy tissue. In contrast, gene therapy can target local expression of desired ion channels to specific regions. Furthermore, ion channel properties can be tailored to be preferentially effective in diseased tissue, even if also expressed in healthy tissue, and to allow adaptation and/or better functionality in the altered microenvironment of an infarct. As a result, it is possible to implement an approach aiming at better preservation of normal CV within the diseased myocardium, thereby opening up an entirely new avenue of antiarrhythmic therapy.[3]

In the ventricle immediately following infarction, there is marked ion channel remodelling[4–6] along with the altered extracellular environment. Remodelling includes inward

* Corresponding author. Tel: +1 212 305 8371; fax: +1 212 305 8780.
E-mail address: rbr1@columbia.edu

currents (Na^+, Ca^{2+}) and connexins affecting CV, and K^+ currents (inward rectifier and transient outward) impacting resting potential, action potential (AP) duration, and refractoriness. Both Na^+ current (I_{Na}) and L-type Ca^{2+} current densities are reduced, and I_{Na} kinetics altered in the central common pathway of the reentrant circuit.[6] Membrane depolarization post-infarction[7] can lead to inactivation of Na^+ channels and, therefore, a further reduction of I_{Na} critical for the propagation. Thus, simply increasing the expression of cardiac Na^+ channel isoform (Nav1.5) may not be an optimal approach in diseased/depolarized tissue. Therefore, we compared the efficacy of over-expression of Nav1.5 with the expression of the non-cardiac skeletal Na^+ channel isoform (SkM1). SkM1 exhibits a less negative voltage-dependent inactivation and faster recovery from inactivation than Nav1.5.[8,9] We hypothesized that the SkM1 expression would result in higher availability of Na^+ channels even in a depolarized post-infarction environment, and thus higher AP upstroke velocity (V_{max}) and improved conduction. We tested this hypothesis in newborn rat ventricle (NBRV) monolayer cultures under normal conditions and during membrane depolarization (elevated external potassium). Our goal was to provide channels with optimized biophysical characteristics to functionally substitute for the remodelled/inactivated native channels, and thus restore normal conduction and prevent or disrupt reentrant circuits. Using gene delivery to increase or restore normal conduction in diseased regions of the heart represents a novel anti-arrhythmic therapy. Our study in an *in vitro* multicellular system provides insight into the therapeutic potential of such an approach and the importance of selecting biophysically optimal ion channel isoforms for the specific underlying substrate.

2. Methods

2.1 Cell culture

One to 2 day old rats were sacrificed and the ventricles removed in accordance with Institutional Animal Care and Use Committee Protocols of Columbia and Stony Brook Universities. These studies conform to the *Guide for the Care and Use of Laboratory Animals (*US National Institutes of Health Publication No. 85–23, revised 1996). Myocytes were isolated using standard enzyme dissociation methods as previously described.[10,11] Cells were studied on days 4–6.

For whole cell patch clamp experiments, cells were plated at normal density, then on the experimental day resuspended with 0.1% trypsin and replated as single cells (voltage clamp) or small clusters (AP) for use within 2–8 h. For syncytial studies of propagating APs or CV, cells were plated onto fibronectin-coated coverslips or multi-electrode arrays (MEAs). The MEA array is an 8×8 grid of 30 μm diameter recording electrodes with 200 or 900 μm inter-electrode spacing.

2.2 Plasmid and viral preparation and gene expression

To increase the TTX sensitivity of the cloned cardiac Na^+ channel, a point mutation (C373Y) was introduced into full-length human Nav1.5 cDNA in the pcDNA3.1 plasmid (provided by Dr Robert Kass, Columbia University). This mutation increases TTX sensitivity without altering gating parameters.[12] The cDNA of the rat skeletal Na^+ channel SkM1 (provided by Dr Gail Mandel, Oregon Health Sciences) was isolated from its original plasmid and inserted into the shuttle vector pDC516, and an adenovirus prepared from this transgene (Admax system, Microbix, Toronto Canada). The titre of the resulting material was determined using fluorescent focus assay (FFA) with mouse anti-adenovirus antiserum (Advanced ImmunoChemical, Long Beach, CA, USA) and goat anti-mouse antiserum (Santa Cruz Biotechnology, Santa Cruz, CA, USA). FFA is an antibody-based titration method which detects only viral particles capable of infecting HEK293 cells. Exogenous genes were expressed in neonatal myocytes by electroporation (Amaxa, Gaithersburg, MD, USA) with ~30–50% efficiency or adenovirus (>90% efficiency),[13] using a multiplicity of infection (MOI) of 20 unless otherwise indicated.

2.3 Single-cell electrophysiological recordings

APs were recorded using a patch electrode in whole cell mode during superfusion at 35°C. Monolayers were used for studying control cultures and resuspended cells for transfected cultures. Transfected cells were selected by GFP fluorescence (co-transfected with separate GFP vector); adenovirus did not require GFP identification due to high expression efficiency. Cultures were compared to those expressing only GFP virus or plasmid. Extracellular and pipette solutions were as previously employed.[13] External solution contained (mmol/L): NaCl 140, KCl 5.4, $CaCl_2$ 1, $MgCl_2$ 1, HEPES 5, glucose 10, adjusted to pH 7.4. Internal solution contained (mmol/L): aspartic acid 130, KOH 146, NaCl 10, $CaCl_2$ 2, EGTA 5, HEPES 10, MgATP 2, (pH 7.2; 295 mOsm). An Axopatch-200B amplifier, digitizer, and pClamp 8 or 9 software (Molecular Devices, Sunnyvale, CA) were used for acquisition and analysis. Stimulation was from a remote extracellular electrode for monolayer studies, and via patch pipette for small clusters.

Voltage clamp was conducted on resuspended cells with temperature 19.0 ± 0.5°C and pipette resistance 1.0–1.5 MΩ for adequate voltage control. Pipette solution contained (mmol/L): CsOH 125, aspartic acid 125, tetraethylammonium chloride 20, HEPES 10, Mg-ATP 5, EGTA 10, and phosphocreatine 3.6 (pH 7.3 with CsOH). After seal formation, stray capacitance was electronically nulled, patch ruptured, and the cell exposed to a low Na^+ solution (mmol/L): NaCl 50, $MgCl_2$ 1.2, $CaCl_2$ 1.8, tetraethylammonium chloride 80, CsCl 5, HEPES 20, glucose 11, 4-aminopyridine 3.0, and $MnCl_2$ 2.0 (pH 7.3 with CsOH). Currents were filtered at 10 kHz and digitized at sampling interval 0.1 ms for whole cell currents and 0.02 ms for capacitative transients.

Whole cell I_{Na} was obtained by subtracting traces elicited with comparable voltage steps containing no current (using pre-pulse holding potential to inactivate Na^+ channels) from raw current traces to eliminate cell capacitance and linear leakage. To examine peak current density, voltage steps (40 ms) from a −100 mV holding potential were imposed from −55 to +45 mV. 'SS' inactivation curve was characterized using a double-pulse protocol: 1000 ms conditioning pulse to various potentials followed by a 40 ms test pulse. To assess how over-expression of different Na^+ channel isoforms affects total Na^+ channel availability, we fit net Na^+ current records to a single Boltzmann equation to derive midpoint $V_{0.5}$ and slope factor *k*. In addition, we found when fitting decay kinetics to a double exponential that the faster component typically represented ~90% of total current. We, therefore, focused on the fast component when comparing kinetics in cells expressing different Na^+ channel isoforms.

2.4 Multicellular functional measurements

Routine measurements of conduction were carried out in MEA dishes during superfusion with physiologic solution (1 mL/min; 35°C). To study drug effects, recordings (spontaneous or stimulated at 2 Hz or ~1.5× spontaneous rate) were made before and during drug exposure and following washout. The data were acquired at 10 kHz with 12 bit precision and analysed as previously described.[14,15] Analysis involved a combination of MSRack software (Multichannel Systems, Reutlingen, Germany), and additional

software provided by Dr Ofer Binah[14] (Technion, Haifa, Israel), which is based on MATLAB and calculates CV maps and other parameters.

Optical mapping of conduction was also employed as previously described.[16] Cells were stained with the calcium-sensitive dye fluo-4 AM (Invitrogen, Carlsbad, CA, USA) excited at 488 nm through fibre optic light guides. Linear CV was assessed in rectangular strips (18 × 7 mm) of myocytes, with a line-pacing electrode at one end to produce simple planar waves (supplementary material online, *Figure S1*). Using a programmable mechanical stage, calcium transients were measured optically with a photomultiplier tube at a precisely measured distance from the stimulating electrode and CV determined based on travel delay from the time of stimulus.[17] Based on this strictly planar wave propagation, effective pathlength for reentry was calculated by simply multiplying CV and calcium transient duration at the highest pacing frequency at which all tested samples showed capture, i.e. 1:1 response.

For recreating anatomical reentry in the dish, we introduced a 1 cm diameter void in the centre of a 25 × 25 cm plastic coverslip using a cloning cylinder during cell plating. Reentry was induced by progressively increasing fast pacing from a point electrode. We mapped propagation using an intensified CMOS camera system with 1280 × 1024 pixel resolution, at a frame rate of 200 fps and a sensor-determined spatial resolution of 22 μm.[17,18] Fluorescent movies of reentrant propagation were collected. For propagation maps, raw data were analysed in custom-developed Matlab software after filtering spatially (Gaussian, 3-pixel kernel) and temporally (Savitsky-Golay, order 2, width 7).

2.5 Chemicals and data analysis

The SkM1 selective blocker μ-conotoxin GIIA (μ-CTX) and tetrodotoxin (TTX) were purchased from Bachem (Torrance, CA, USA) and Calbiochem (Gibbstown, NJ, USA), respectively. Statistical analysis was by *t*-test or ANOVA, as indicated and $P < 0.05$ taken as significant; data are expressed as mean ± SEM.

3. Results

3.1 Na^+ channel-dependent conduction in newborn rat ventricle cell cultures

We have previously reported that V_{max} and resting potential are constant from days 2–8 in culture.[19] *Figure 1* illustrates that CV also is stable during days 4–6, studied here. Although we previously reported the presence of I_{Na} and TTX sensitive APs in these cultures,[20,21] others have reported only slow, Na-independent APs.[22] Therefore, we confirmed the dependence of V_{max} and CV on I_{Na} in our monolayers by measuring the effect of TTX on both parameters. As illustrated in the supplementary material online, *Figure S2*, V_{max} was markedly reduced by TTX. On average, V_{max} decreased from 142.4 ± 11.5 ($n = 10$) to 61.9 ± 13.6 V/s ($n = 5$) after 1 μmol/L TTX ($P < 0.05$). AP amplitude also decreased (from 122.6 ± 2.0 to 115.5 ± 0.8; $P < 0.05$). Consistent with these AP effects, TTX reduced CV as measured from activation maps. In 1 μmol/L TTX, CV decreased from 28.5 ± 0.8 to 19.9 ± 0.9 cm/s ($n = 4$; $P < 0.05$). In contrast, 100 nmol/L TTX only decreased CV ~10%. Combined with the absence of a significant effect of 100 nmol/L TTX on endogenous I_{Na} (*Figure 2*), this indicates that the contributing Na^+ channel is largely the TTX-resistant cardiac isoform in NBRV cultures.

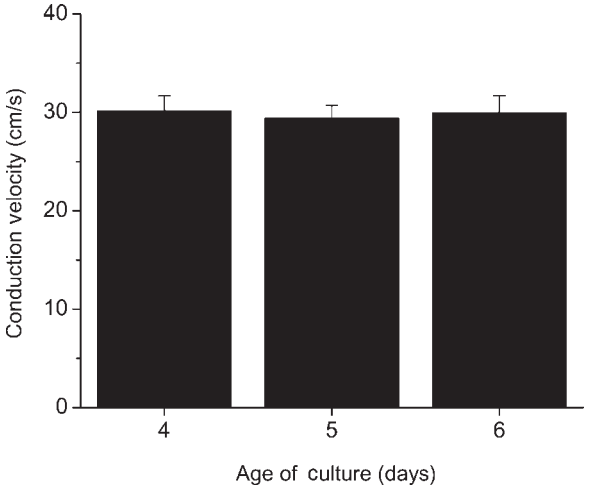

Figure 1 Conduction velocity is constant during culture. Myocytes were plated and maintained in monolayer culture on MEA substrate. At the indicated times, electrograms were recorded (35°C superfusion with 5.4 mmol/L K^+ solution) and CV calculated (see Methods and supplementary material online); $n = 21$, 16, 6 at days 4, 5, 6, respectively.

3.2 Gene delivery of Na^+ channel isoforms in newborn rat ventricle cell cultures

We next used a plasmid expressing SkM1 and another expressing Nav1.5 with a point mutation (Nav1.5-C373Y) to achieve similar sensitivity as SkM1 to TTX (nanomolar block). We asked if, using electroporation, we could express these genes in NBRV and measure TTX sensitive I_{Na} in excess of endogenous current. Low TTX (100 nmol/L) was used to confirm expression of TTX-sensitive isoforms (*Figure 2A*). The representative traces show greater peak current when either Na^+ channel is expressed, and faster decay time course with SkM1 than with Nav1.5-C373Y. When measured at each cell's peak current, the average fast time constant of decay in SkM1 and Nav1.5-C373Y cells is 1.13 ± 0.05 and 1.63 ± 0.06 ($n = 30$, 15; $P < 0.05$). The mean peak net I_{Na} density (*Figure 2B*, left) in GFP expressing cells is significantly less ($P < 0.05$) than that of either SkM1 or Nav1.5-C373Y expressing cells. In a subset of cells (*Figure 2B*, right), 100 nmol/L TTX was used to pharmacologically ablate expressed current. There is no significant effect in GFP cells but a significant decrease with Nav1.5-C373Y or SkM1; after TTX, the three groups do not differ statistically, indicating no significant downregulation of native I_{Na} by Nav1.5-C373Y or SkM1 expression.

3.3 Functional benefits of non-native Na^+ channel isoform in newborn rat ventricle cultured cells

To mimic the depolarized milieu that can occur post-infarction, we determined if Na^+ channel over-expression successfully preserves V_{max} in elevated external K^+. In control, non-transfected monolayer cultures, increasing external K^+ from 5.4 to 10 mmol/L depolarized the resting potential from −75.1 ± 1.1 to −57.8 ± 1.1 mV ($n = 8$). Studies in transfected cells (*Figure 3*) demonstrate that SkM1 is more effective than Nav1.5-C373Y in preserving V_{max} in K^+ depolarized myocytes. SkM1 increased V_{max} in both normal and high K^+ Tyrode compared to GFP; Nav1.5-C373Y provided no benefit in high K^+ compared to GFP. In addition, we observed no difference in AP amplitude or duration, or on L-type Ca^{2+} current magnitude in SkM1 vs. GFP cells (data not shown). To further confirm that the SkM1 expression was the cause of the protective effect in high K, a separate series of SkM1 and GFP expressing cells ($n = 7$ of each) were first

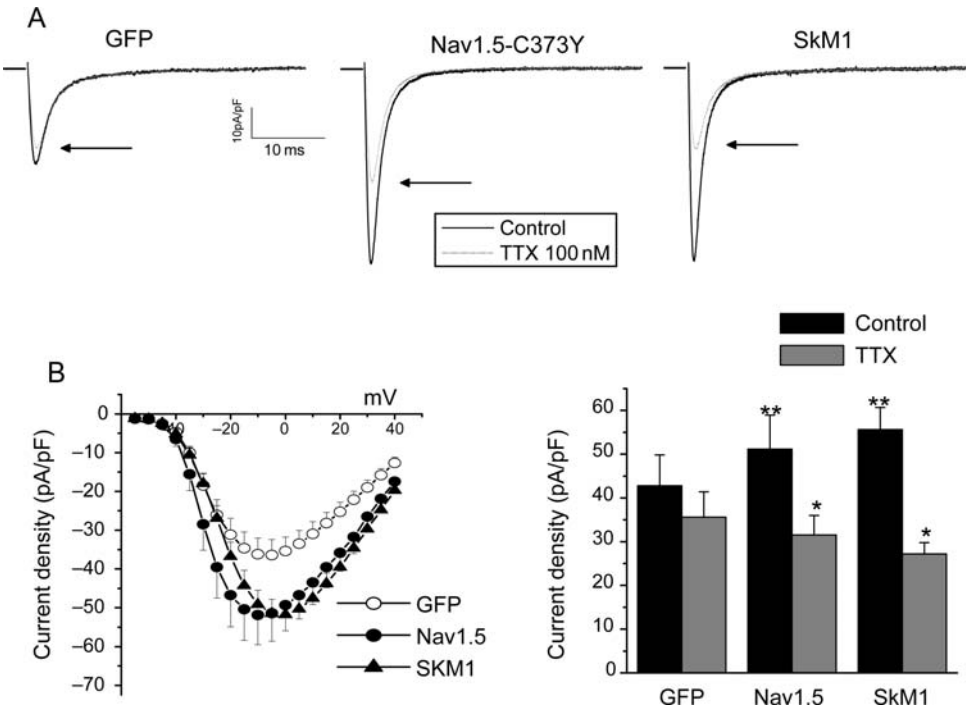

Figure 2 Characteristics of Na^+ current following transfection with different channel isoforms. (*A*) Representative current traces from an isolated cell transfected with GFP (left), Nav1.5-C373Y (middle), and SkM1 (right). Currents were recorded for a step from −100 mV holding potential to the peak of the I–V relation under control conditions (solid black trace) and in 100 nmol/L TTX (dotted gray trace). Arrows indicate peak current in TTX. (*B*) Mean I–V relations for the corresponding transfection conditions (left; $n = 29$, 15, and 33, respectively) show peak current for Nav1.5-C373Y and SkM1 significantly greater than GFP. Peak current measured in subset of cells (right) before and after 100 nmol/L TTX; $n = 12$ for GFP; 11 for others; $^*P < 0.05$ relative to matched control; $^{**}P < 0.05$ relative to GFP. Values in bar graph were measured from the peak of the average I–V relation in each condition (−10 mV in GFP and Nav1.5 control; 0 mV in SkM1 control; −5 mV in all after TTX).

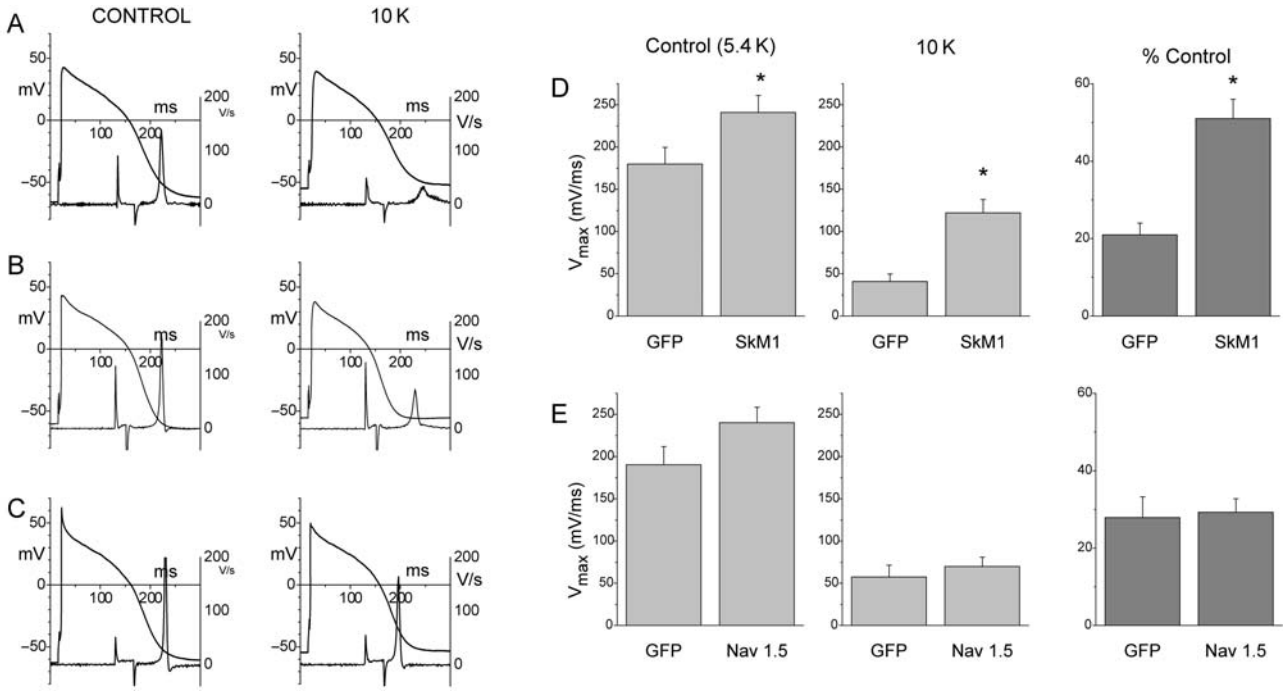

Figure 3 Effect of depolarizing the membrane at rest (by increasing external K) on AP upstroke. (*A*) AP and its first derivative (on an offset, 10x expanded, time scale) from a GFP transfected cell cluster, in 5.4 (*left*) and 10 mmol/L external K^+ (*right*). (*B* and *C*) Similar records from Nav1.5-C373Y and SkM1 transfected clusters, respectively. All cells paced at 1 Hz. (*D* and *E*) SkM1 but not Nav1.5 expression is protective of AP upstroke in K^+ depolarized cells. *Left*: Mean data comparing V_{max} in GFP and SkM1 (D) or Nav1.5-C373Y (Nav1.5, E) cells. In each case, Na^+ channel cells were matched to GFP expressing cells from same preparation. *Middle*: mean data from same cells after raising K^+ from 5.4 to 10 mmol/L. *Right*: Mean data on inhibition (as % control) of V_{max} by elevated K^+ illustrating the protective effect of SkM1 but not Nav1.5 in comparison to GFP. $^*P < 0.05$ vs. GFP. In (D), $n = 10$ for both GFP and SkM1 groups; in (E), $n = 10$ and 13 for GFP and Nav1.5-C373Y, respectively.

exposed to 100 nmol/L TTX, then to elevated K^+ in continued TTX. Low TTX significantly reduced V_{max} in the SkM1 group (from 215 ± 13 to 181 ± 13 V/s, $P < 0.05$), but not the GFP group (186 ± 19 to 171 ± 18 V/s, $P > 0.05$). In low TTX and high K^+ conditions, V_{max} did not differ between groups (V_{max} in 10 mmol/L K^+ 34 ± 6 and 37 ± 7% of normal K^+ TTX values, for SkM1 and GFP, respectively; $P > 0.05$) In short, the protective effect of SkM1 was absent in 100 nmol/L TTX.

3.4 SkM1-augmented conduction in newborn rat ventricle cultured cardiomyocyte monolayers

Based on these results, we prepared an adenovirus of SkM1 to study syncytial properties during spatially homogeneous expression. To ensure selective pharmacological block of expressed SkM1, in some studies we used μ-CTX GIIIA (μ-CTX), which selectively blocks rat SkM1 channels with no effect on native I_{Na} in NBRV cells (*Figure 4A* and *B*). In separate experiments, we confirmed that 1000 nmol/L μ-CTX was a saturating concentration, showing comparable effects to 500 nmol/L on cells with expressed SkM1 current, while having no effect on control cells (data not shown). Viral expression of SkM1 resulted in increased net I_{Na} (*Figure 4C*). In addition, both the midpoint (−68.0 ± 1.5 mV) and slope factor (6.6 ± 0.4 mV) of steady-state inactivation in SkM1 myocytes differed significantly from those in GFP cells (−73.8 ± 1.8 and 5.1 ± 0.2 mV). After exposure to 100 nmol/L TTX (to selectively block expressed current), this difference was eliminated due to a significant shift in the midpoint of the SkM1 curve (*Figure 4D*). *Figure 5* illustrates that SkM1 expressing cells also had faster kinetics at all voltages compared to control GFP cells. After μ-CTX block of the expressed current, kinetics of the residual (endogenous) current in SkM1 expressing cells was equivalent to that of GFP cells. Finally, we calculated the μ-CTX sensitive current, representing just expressed SkM1 channels. As expected, decay kinetics were faster than the net current in SkM1 expressing cells, which represents a mix of exogenous and endogenous Na^+ channels.

Based on the Boltzmann fit to the inactivation relations (*Figure 4D*), the relative Na^+ channel availability in high K^+ (−58 mV) is 0.18 and 0.04 for SkM1 and GFP cells, respectively, which should provide marked CV protection in the case of SkM1 expression. We, therefore, next examined how SkM1 expression affects CV in depolarized tissue. First, we confirmed a dose-dependent efficacy of viral treatment on CV. At MOI 10, 100 nmol/L TTX did not significantly reduce CV (11% decrease, $n = 4$; $P > 0.05$), but at MOI 20, it reduced CV by 33% ($n = 6$; $P < 0.05$), reflecting the larger contribution of expressed SkM1 channels at the higher MOI. The contribution of expressed channels to CV at MOI 20 is illustrated in *Figure 6A*. Low TTX had a more pronounced effect on CV in SkM1 than control GFP cultures, indicating the expressed current contributes to AP upstroke and CV. Further, in SkM1 cultures, there was no significant effect of 10 mmol/L K^+ on CV, while K^+ elevation reduced CV in control cultures significantly (*Figure 6B*). Pharmacological ablation of the expressed current with μ-CTX made CV in SkM1 cultures much more sensitive to high K^+ (similar reduction in CV to control samples).

We further tested if the beneficial effects of SkM1 extended over a range of pacing frequencies (CV restitution relation, *Figure 7A*). Using multiple regression or 3-way ANOVA, we found that all three factors (frequency, high

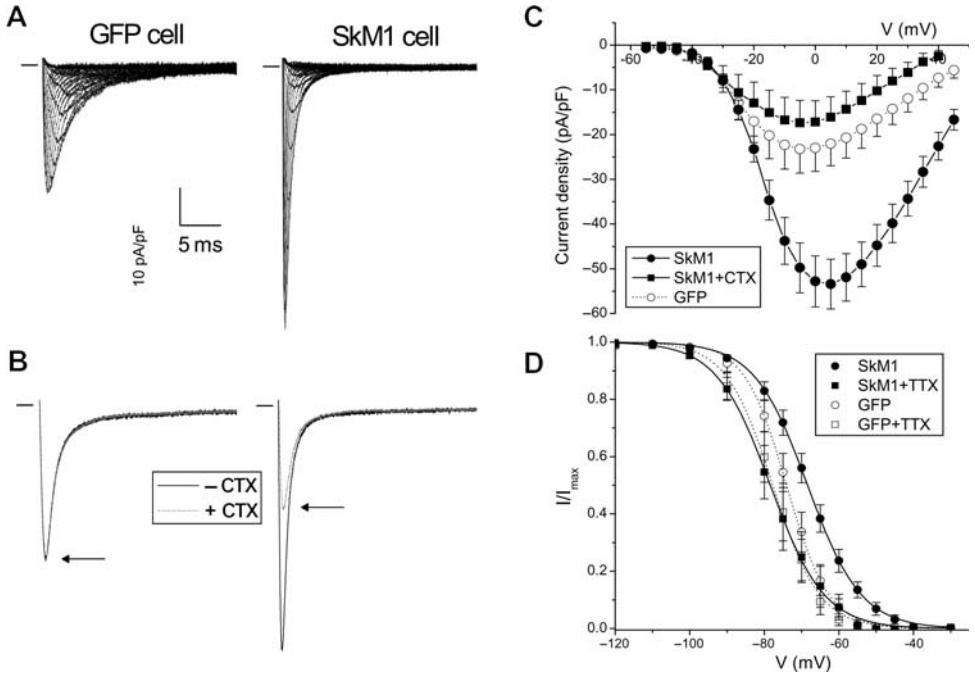

Figure 4 Characteristics of I_{Na} following exposure to GFP or SkM1 expressing adenoviruses. (*A*) Family of current traces with voltage steps from −55 to +40 mV from an isolated cell expressing GFP (*left*) or SkM1 (*right*). (*B*) Effect of 1000 nmol/L μ-CTX on a single current trace (from −100 mV holding potential to peak of I–V relation) in another GFP and SkM1 expressing cell. The traces following μ-CTX are shown as dashed gray lines, with the peaks marked by arrows; μ-CTX did not affect the GFP cell but reduced current in the SkM1 cell, where total I_{Na} is a combination of native and expressed current. (*C*) Mean I–V relation of I_{Na} in SkM1 cells before ($n = 34$) and after ($n = 7$) exposure to μ-CTX to block expressed current; also shown is mean I–V in separate set of GFP expressing cells ($n = 13$). (*D*) Na^+ current inactivation relation is shifted in SkM1 expressing myocytes. The inactivation relation is shown for SkM1 and GFP cultures before and after the exposure of 100 nmol/L TTX.

K^+, and SkM1) had a statistically significant effect on CV. In particular, SkM1 treatment increased CV compared to GFP controls ($P = 0.001$). In the absence of pronounced effects of SkM1 on AP duration, this faster linear CV results in a projected longer pathlength for completion of a reentrant circuit. This holds true even at higher frequencies, as typically encountered in a reentrant rhythm (*Figure 7B*). In fact, wavelength values with SkM1 are higher than those with GFP in each condition, such that in high K^+ conditions the presence of SkM1 results in wavelength levels comparable to controls in normal K^+.

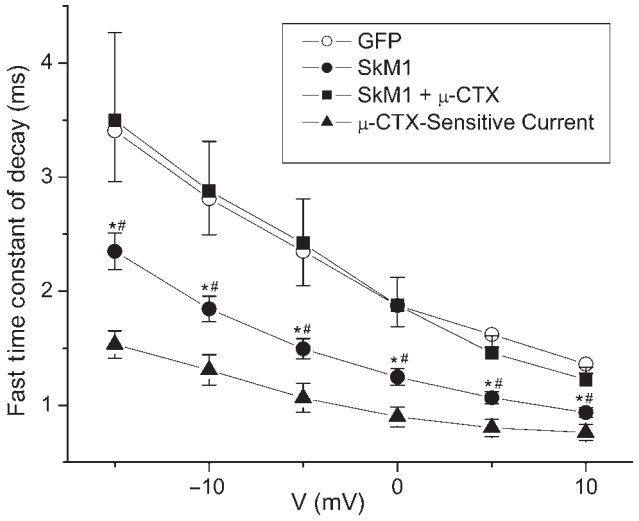

Figure 5 Decay kinetics of expressed and native Na^+ current in isolated cells. The fast time constant of current decay is plotted as a function of voltage in GFP and SkM1 expressing cultures. The currents in SkM1 cultures reflect a sum of expressed and native components; *indicates $P < 0.05$ for SkM1 relative to GFP. μ-CTX was then used to block the expressed current in SkM1 cells and the residual (endogenous) current exhibited kinetics indistinguishable from those of GFP cells; #indicates $P < 0.05$ for SkM1 relative to SkM1+μ-CTX. In addition, the μCTX-sensitive current (SkM1 current minus SkM1+ μ-CTX current) also was fit to determine the time constants for the expressed SkM1 current after removal of contaminating endogenous current. For GFP, SkM1, SkM1+μ-CTX, and μ-CTX-sensitive plots, $n = 10$, 34, 9, and 7, respectively.

To examine reentry dynamics after SkM1 expression rather than extrapolate from planar wave behaviour, we induced reentry with progressively increasing pacing from a point electrode in a culture containing a large void. In both normal and high K^+, the angular velocity (AV) of induced reentry was faster in SkM1 cultures compared to GFP control (*Figure 8A*). In the representative GFP sample shown, the excitation wave completes one circuit in normal K^+ (black line marks wavefront, top row) in ~0.5 s. Raising K^+ to 10 mmol/L slows AV by 40% (2nd row). In contrast, in the SkM1 culture, AV is faster in normal K, completing one circuit in ~4/5 time, while in high K^+ AV of the SkM1 culture is equivalent to that of control (GFP) culture in normal K^+. In addition, the excitable gap, as indicated by the diastolic interval (*Figure 8B* and *C*) is shorter in SkM1 than GFP cultures. ANOVA for the DI data, in which two factors are considered, [K^+] and SkM1 treatment, yields $P < 0.02$ for both factors. That is, both [K^+] and treatment can induce significant change in DI. Both the faster AV and shorter excitable gap are expected to facilitate reentry self-termination.

4. Discussion

Exogenous expression of the cardiac isoform, Nav1.5, and a skeletal isoform, SkM1, selected based on its biophysical properties, demonstrated clear benefits of SkM1 in preserving V_{max} in K^+-depolarized myocytes. At the syncytium level, SkM1 expression resulted in superior maintenance of CV during K^+-depolarization, compared to GFP control. Studies of reentry around a void confirmed maintenance of high AV and a short excitable gap in K^+-depolarized cultures when SkM1 was expressed. These characteristics would be expected to facilitate reentry self-termination, which is supported by a preliminary study[23] in a canine model of myocardial infarction in which SkM1 adenovirus was injected into the epicardial border zone at the time of occlusion. Five days later, the electrograms were narrower than those of hearts not receiving SkM1. In addition, premature stimulation

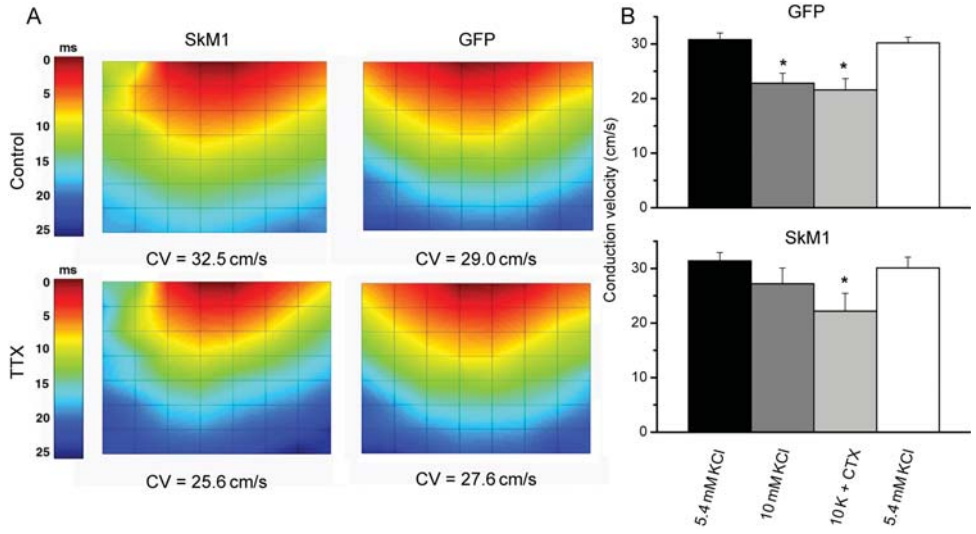

Figure 6 Expressed SkM1 current contributes to CV and protects against K^+ depolarization. (*A*) Representative activation maps from monolayer cultures show 100 nmol/L TTX reduces CV of SkM1, but not GFP expressing culture. (*B*) Mean data showing protective effect of SkM1 on CV in K^+ depolarized cultures. 10 mmol/L K^+ significantly reduced CV in GFP but not SkM1 cultures. μ-CTX in high K^+ had no further effect in GFP cultures but reduced CV in SkM1 cultures to the equivalent level of GFP cultures. All effects fully reversible; $n = 6$ for each group.

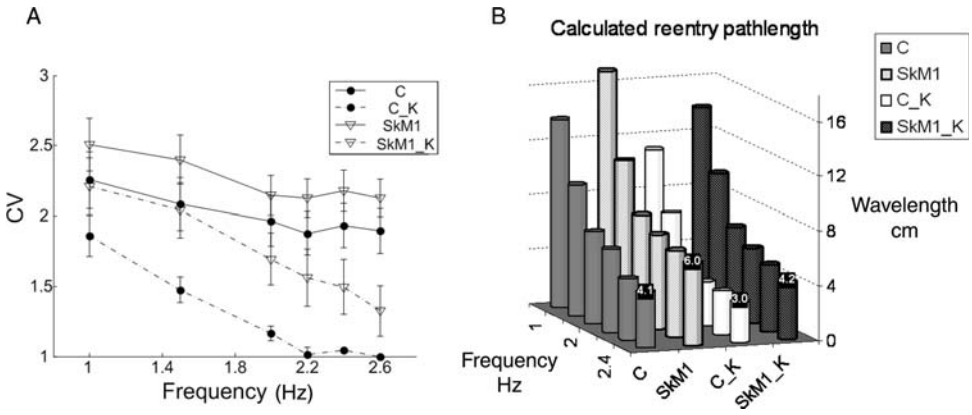

Figure 7 SkM1 expression increases effective pathlength for reentry at all frequencies in both normal and elevated K^+ in monolayer cultures. (*A*) CV data (normalized to lowest value) for planar waves in control (GFP) and SkM1 expressing cultures in normal (solid lines) and high K^+ (dashed lines) over a range of pacing frequencies common to all cultures ($n = 24$ per group). SkM1 cultures maintain higher CV under normal and high K^+ conditions, $P < 0.02$ by n-way ANOVA; no significant difference was found for CV in normal K^+ between control and SkM1 for individual frequencies. (*B*) Estimated wavelength over a frequency range for the four experimental groups; the indicated numbers (in cm) show the minimum effective pathlength for reentry based on wavelength calculations at 2.6 Hz. For normal and depolarized tissue conditions, the SkM1 samples require larger space for the initiation of a reentrant wave ($P < 0.01$ by n-way ANOVA and multiple regression). Data collected at 30°C.

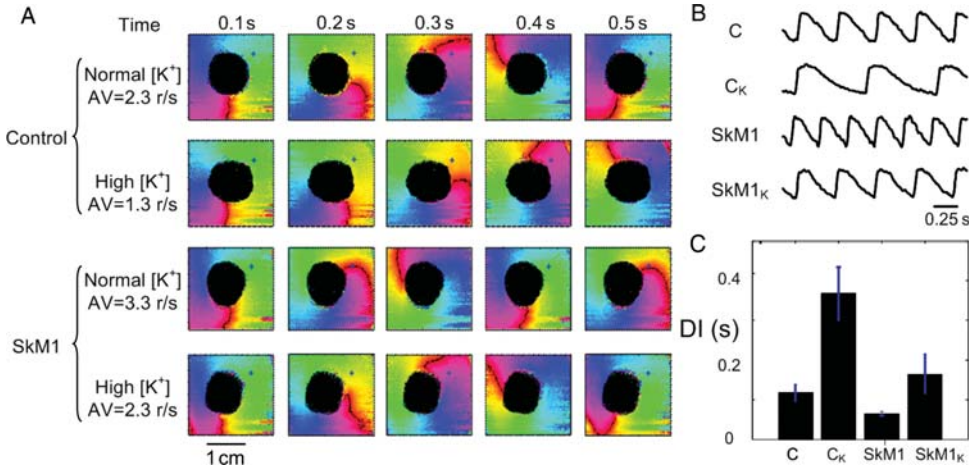

Figure 8 During sustained anatomical reentry (1 cm obstacle), SkM1 expressing monolayer culture exhibits faster rotation (AV, angular velocity). (*A*) Example of reentry in GFP and SkM1 cultures in normal and high K. (*B*) Example calcium traces, indicating difference in refractory period (diastolic interval, DI) during the four reentrant cases. (*C*) Bar graph summarizes DI data ($n = 7$, 4 cultures). Multiple spatial points were used from an annulus around the void. Data collected at 25°C.

induced VT/VF in all control post-infarction animals but produced only three to five beat VT bursts in the SkM1-treated animals.

The greater benefit attained by SkM1 rather than Nav1.5 expression in preserving V_{max} during K^+ depolarization was not due to differences in expression, since peak current following either treatment was equivalent. Further, the residual TTX-resistant native current following exposure to 100 nmol/L TTX was comparable in all groups, indicating that the expression of neither isoform resulted in significant down regulation of native Nav1.5. Rather, the benefit of SkM1 expression can be ascribed to its effect on the position of the total current steady-state inactivation relation, which in the presence of SkM1 is significantly shifted toward positive voltages relative to GFP expressing control cells. While the SkM1 inactivation relation can be affected by the protocol holding potential,[24,25] our results with selective toxins on both AP and CV demonstrate that SkM1 channels were available and functional in these myocytes. Finally, in addition to the position of the steady-state inactivation relation, the faster recovery from inactivation of SkM1[9] also may contribute to Na^+ channel availability in the SkM1-treated cultures, particularly at rapid pacing rates or during reentrant rhythms. This leads to a shift in the occurrence of alternans (other instabilities or block of propagation) towards higher frequencies (data not shown), and better maintenance of normal propagation.

Existing therapies for treating reentrant arrhythmias are largely restricted to decreasing/blocking conduction and/or prolonging refractoriness, and the available tools are either ablation or ion channel blockers, with some recent exceptions where remodelling of the substrate was attempted.[26] Ablation has the advantage of being targeted to specific sites, but is invasive, permanently scars tissue, and is not without complications. Global pharmacologic ion channel blockade can be proarrhythmic.[27] Drug effects on otherwise healthy tissue exacerbate these problems. The gene therapy approach employed here has the advantage of potentially being locally applied to target diseased regions. For example, in extensive mapping studies of

human subjects with ischaemic heart disease, Reddy *et al*.[28] demonstrated they could identify sites of fragmented electrogram configuration, reflecting abnormal conduction, and ablate these to reduce the number of ICD shocks (for lethal arrhythmias) by about 70%. A gene therapy approach would use the same approach but inject the constructs at those sites of fragmented activity to improve conduction. Further, constructs can be designed to be preferentially effective in diseased tissue, even if also expressed in healthy tissue. By rescuing conduction in the diseased heart with an altered microenvironment, this approach presents a conceptually new antiarrhythmic therapy, where a search for biophysically optimized proteins, not necessarily native to the heart, may yield highly desirable functional benefits.

4.1 Limitations

Caution is required in extrapolating from the K^+-depolarized monolayer model studied here to the intact, diseased myocardium. In the latter situation, there are metabolic, electrophysiologic, and other abnormalities (e.g. hypoxia, acidosis) that could impact the function and/or efficacy of expressed SkM1 channels. Further, gap junctional changes[29] may contribute to conduction deficiencies, and the effectiveness of Na^+ channel over-expression in that setting remains to be determined.

Supplementary material

Supplementary material is available at *Cardiovascular Research* online.

Conflict of interest: none declared.

Funding

This work was supported by a National Institutes of Health Program Project Grant [HL-28958].

References

1. Allessie MA, Boyden PA, Camm AJ, Kleber AG, Lab MJ, Legato MJ *et al*. Pathophysiology and prevention of atrial fibrillation. *Circulation* 2001; **103**:769–777.
2. Wit AL, Janse MJ. *The Ventricular Arrhythmias of Ischemia and Infarction, Electrophysiological Mechanisms*. Mt. Kisco, Futura Publishing; 1993.
3. Rosen MR, Brink PR, Cohen IS, Danilo P Jr, Robinson RB, Rosen AB *et al*. Regenerative therapies in electrophysiology and pacing. *J Interv Card Electrophysiol* 2008;**22**:87–98.
4. Pinto JM, Boyden PA. Electrical remodeling in ischemia and infarction. *Cardiovasc Res* 1999;**42**:284–297.
5. Wasson S, Reddy HK, Dohrmann ML. Current perspectives of electrical remodeling and its therapeutic implications. *J Cardiovasc Pharmacol Ther* 2004;**9**:129–144.
6. Baba S, Dun W, Cabo C, Boyden PA. Remodeling in cells from different regions of the reentrant circuit during ventricular tachycardia. *Circulation* 2005;**112**:2386–2396.
7. Spear JF, Michelson EL, Moore EN. Cellular electrophysiologic characteristics of chronically infarcted myocardium in dogs susceptible to sustained ventricular tachyarrhythmias. *J Am Coll Cardiol* 1983;**1**: 1099–1110.
8. Zhang Y, Hartmann HA, Satin J. Glycosylation influences voltage-dependent gating of cardiac and skeletal muscle sodium channels. *J Membr Biol* 1999;**171**:195–207.
9. Bennett ES. Channel activation voltage alone is directly altered in an isoform-specific manner by Na(v1.4) and Na(v1.5) cytoplasmic linkers. *J Membr Biol* 2004;**197**:155–168.
10. Protas L, Robinson RB. Neuropeptide Y contributes to innervation-dependent increase in $I_{Ca,L}$ via ventricular Y2 receptors. *Am J Physiol* 1999;**277**:H940–H946.
11. Yin L, Bien H, Entcheva E. Scaffold topography alters intracellular calcium dynamics in cultured cardiomyocyte networks. *Am J Physiol Heart Circ Physiol* 2004;**287**:H1276–H1285.
12. Satin J, Kyle JW, Chen M, Bell P, Cribbs LL, Fozzard HA *et al*. A mutant of TTX-resistant cardiac sodium channels with TTX- sensitive properties. *Science* 1992;**256**:1202–1205.
13. Qu J, Barbuti A, Protas L, Santoro B, Cohen IS, Robinson RB. HCN2 overexpression in newborn adult ventricular myocytes: distinct effects on gating excitability. *Circ Res* 2001;**89**:e8–e14.
14. Meiry G, Reisner Y, Feld Y, Goldberg S, Rosen M, Ziv N *et al*. Evolution of action potential propagation and repolarization in cultured neonatal rat ventricular myocytes. *J Cardiovasc Electrophysiol* 2001;**12**:1269–1277.
15. Binah O, Dolnikov K, Sadan O, Shilkrut M, Zeevi-Levin N, Amit M *et al*. Functional and developmental properties of human embryonic stem cells-derived cardiomyocytes. *J Electrocardiol* 2007;**40**:S192–S196.
16. Bien H, Yin L, Entcheva E. Calcium instabilities in mammalian cardiomyocyte networks. *Biophys J* 2006;**90**:2628–2640.
17. Chung CY, Bien H, Entcheva E. The role of cardiac tissue alignment in modulating electrical function. *J Cardiovasc Electrophysiol* 2007;**18**: 1323–1329.
18. Entcheva E, Bien H. Macroscopic optical mapping of excitation in cardiac cell networks with ultra-high spatiotemporal resolution. *Prog Biophys Mol Biol* 2006;**92**:232–257.
19. Robinson RB. Action potential characteristics of rat cardiac cells do not change with time in culture. *J Mol Cell Cardiol* 1982;**14**:367–370.
20. Zhang JF, Robinson RB, Siegelbaum SA. Sympathetic neurons mediate developmental change in cardiac sodium channel gating through long-term neurotransmitter action. *Neuron* 1992;**9**:97–103.
21. Robinson RB, Legato MJ. Maintained differentiation in rat cardiac monolayer cultures: Tetrodotoxin sensitivity and ultrastructure. *J Mol Cell Cardiol* 1980;**12**:493–498.
22. Schanne OF, Ruiz-Ceretti E, Rivard C, Chartier D. Determinants of electrical activity in clusters of cultured cardiac cells from neonatal rats. *J Mol Cell Cardiol* 1977;**9**:269–283.
23. Sosunov EA, Anyukhovsky EP, Danilo P Jr, Rosen TS, Shlapakova IN, Duffy HS *et al*. Transfecting the skeletal muscle sodium channel, Skm1, into infarct border zone increases V_{Max}, normalizes activation and is antiarrhyhmic. (Abstract). *Heart Rhythm* 2008;**5**:S115.
24. Filatov GN, Pinter MJ, Rich MM. Resting potential-dependent regulation of the voltage sensitivity of sodium channel gating in rat skeletal muscle in vivo. *J Gen Physiol* 2005;**126**:161–172.
25. Ji S, Sun W, George AL Jr, Horn R, Barchi RL. Voltage-dependent regulation of modal gating in the rat SkM1 sodium channel expressed in Xenopus oocytes. *J Gen Physiol* 1994;**104**:625–643.
26. Nattel S, Shiroshita-Takeshita A, Brundel BJ, Rivard L. Mechanisms of atrial fibrillation: lessons from animal models. *Prog Cardiovasc Dis* 2005;**48**:9–28.
27. The Sicilian gambit. A new approach to the classification of antiarrhythmic drugs based on their actions on arrhythmogenic mechanisms. Task Force of the Working Group on Arrhythmias of the European Society of Cardiology. *Circulation* 1991;**84**:1831–1851.
28. Reddy VY, Reynolds MR, Neuzil P, Richardson AW, Taborsky M, Jongnarangsin K *et al*. Prophylactic catheter ablation for the prevention of defibrillator therapy. *N Engl J Med* 2007;**357**:2657–2665.
29. Peters NS, Coromilas J, Severs NJ, Wit AL. Disturbed connexin43 gap junction distribution correlates with the location of reentrant circuits in the epicardial border zone of healing canine infarcts that cause ventricular tachycardia. *Circulation* 1997;**95**:988–996.